Diffusion in lattice Lorentz gases with a percolation threshold

L. Acedo and A. Santos
Departamento de Física, Universidad de Extremadura, E-06071 Badajoz, Spain
(Received 19 January 1999)

A mean-field approximation for the diffusion coefficient in lattice Lorentz gases with an arbitrary mixture of pointlike stochastic scatterers in the low-density limit is proposed. In this approximation, the diffusion coefficient is directly related to the first return probability of the moving particle in the corresponding Cayley tree through an effective ring operator. A renormalization scheme for the approximate determination of the first return probability is constructed. The predictions of this mean-field theory and those of the repeated ring approximation (RRA) are compared with computer simulation results for models in which a fraction x_B of the scatterers are deterministic backscatterers, so that the diffusion coefficient vanishes beyond a certain percolation threshold x_B^c. The approximation proposed in this paper is seen to be in good agreement with the simulation results, in contrast to the RRA, which already fails to give the correct percolation threshold. [S1063-651X(99)10807-9]

PACS number(s): 05.20.−y, 05.40.−a, 51.10.+y

I. INTRODUCTION

Lattice Lorentz gases have been often used as simple models for nonequilibrium statistical-mechanical systems [1,2]. Moreover, they have recently been studied from the point of view of the dynamical systems theory in order to analyze the connection between the macroscopic transport properties, such as the diffusion coefficient, and the chaos properties of the microscopic dynamics [3]. In a lattice Lorentz gas, a particle follows ballistic trajectories on a d-dimensional regular lattice with a fraction ρ of the sites occupied by fixed scatterers randomly distributed. Upon hitting a scatterer, the moving particle modifies its direction of motion according to a given set of stochastic (or deterministic) collision rules depending on the type of scatterer. An example of a lattice Lorentz gas is the rotator model [4], in which a fraction x_R of the scatterers are stochastic right rotators, a fraction x_L are stochastic left rotators, and a fraction $x_B=1-x_R-x_L$ are deterministic backscatterers. The scatterers that we will consider in this paper are pointlike, but other models with excluded volume scatterers have also been defined [4,5].

The main transport property in Lorentz gases is the diffusion coefficient $D(\rho)$, which is defined by the Einstein relation

$$\langle r^2(t)\rangle \approx 2dD(\rho)t, \quad t\to\infty, \tag{1.1}$$

where the system has been assumed isotropic. In the case of lattice Lorentz gases, the Green-Kubo formula for the diffusion coefficient reads

$$D(\rho)=\frac{1}{d}\left(\sum_{t=0}^{\infty}\Phi(t)-\frac{1}{2}\right), \tag{1.2}$$

where

$$\Phi(t)=\langle \mathbf{v}(t)\cdot\mathbf{v}(0)\rangle \tag{1.3}$$

is the velocity autocorrelation function. The brackets in Eqs. (1.1) and (1.3) denote an average over different trajectories in a given lattice realization, followed by a subsequent average over different realizations. The discrete nature of these models gives rise to an important difference with respect to the continuous case, making the prediction for D in the Boltzmann approximation incorrect even in the low-density limit ($\rho\to 0$) [6]. The reason for this is the contribution of correlated sequences of collisions appearing in any discrete model with backscattering, which gives rise to one-dimensional pathologies. The contribution associated with these correlated trajectories has not been evaluated in general, except for some particular models. For example, van Beijeren and Ernst [7] used an analytical enumeration method to derive the exact expression for the diffusion coefficient in the case of *identical* point scatterers on a Bethe lattice or Cayley tree. In the case of the rotator model on the square lattice with $x_R=1$ or $x_L=1$, the exact result becomes

$$D(\rho)=\frac{1}{2\rho}\left(\mathrm{Re}\,\frac{1}{1-\omega_1}-\frac{x}{1+x}-\frac{\rho}{2}\frac{1-x}{1+x}\right), \tag{1.4}$$

where x is the first return probability, which is obtained from the cubic equation

$$1=2\,\mathrm{Re}\,\frac{x+\omega_1}{1+x\omega_1}+\frac{x-\omega_2}{1-x\omega_2}. \tag{1.5}$$

In these equations, ω_1 and ω_2 are eigenvalues of the collision matrix W_{ij} (See Sec. II). Recently, van Beijeren has also found the exact diffusion coefficient for the *deterministic* rotator model on a Cayley tree [8]:

$$D(\rho)=\frac{(1-x)^2}{2\rho}\left[\frac{1}{1-x(1-x_B)}-\frac{\rho}{2}\right], \tag{1.6}$$

where the probability of first return is now given by the following cubic equation [9]:

$$x=x_B+(1-x_B)x^3. \tag{1.7}$$

Equation (1.7) predicts that $x=1$ (absence of percolation) if the fraction of pure backscatterers is equal to or larger than a critical value $x_B^c=\frac{2}{3}$ [9,10]. Beyond this percolation threshold, the particle becomes trapped in a finite cluster of ends blocked by backscatterers; as a consequence, the diffusion coefficient vanishes (absence of diffusive percolation). As x_B goes to x_B^c from below, Eqs. (1.6) and (1.7) show that D vanishes as

$$D\sim(x_B^c-x_B)^{\mu} \tag{1.8}$$

with a critical exponent $\mu=2$.

The threshold value $x_B^c=\frac{2}{3}$ must also be correct in the case of *stochastic* rotators, according to the following argument [8,11]. A nonpercolating cluster consists of a collection of bonds with nodal points at the locations of the rotators, bounded in all directions by pure backscatterers. Consequently, the precise nature of the rotators is unimportant, as long as they allow a returning particle to explore all directions from the nodal point. It is then appealing to look for an approximate simple relationship between the diffusion coefficient and the probability of first return in lattice Lorentz gases with a percolation threshold. This is one of the primary objectives of this paper.

An analytical approximation for the reduced low-density diffusion coefficient $D^*\equiv\lim_{\rho\to 0}\rho D(\rho)$ of any model with a mixture of scatterers was given by Ossendrijver, Santos, and Ernst [4] by resumming all the contributions associated with the so-called repeated ring collisions. The low-density diffusion coefficient given by the repeated ring approximation (RRA) coincides with the exact result of van Beijeren and Ernst in the case of identical point scatterers [7]. In Ref. [12] we showed (by means of Monte Carlo simulations) that this approximation is also exact in models without pure backscatterers (for instance, including only symmetric species of right and left rotators or right and left mirrors). Nevertheless, the prediction of the RRA for any model that includes pure backscatterers was shown to be very poor, except if $x_B\ll 1$. In particular, this approximation predicts a diffusive percolation threshold $x_B^c=\frac{1}{3}$ for models defined on the square lattice, while the simulations indicate $x_B^c=\frac{2}{3}$.

The aim of this paper is to propose a new mean-field theory for the diffusion coefficient in a Cayley-tree lattice Lorentz gas with a mixture of point scatterers. This theory keeps the excellent predictions of the RRA for the case of identical point scatterers and also in the absence of backscatterers, but clearly improves the latter theory for percolation models. It will be shown that the proposal made in this paper predicts a percolation threshold $x_B^c=\frac{2}{3}$ ($x_B^c=\frac{4}{5}$) for any stochastic rotator or mirror model with backscatterers defined on the square (hexagonal) lattice. This prediction is in excellent agreement with our Monte Carlo simulation results. The theory is constructed upon the assumption that the relationship between the ring operator R and the first return probability matrix X that Ossendrijver *et al.* [4] found for identical scatterers, $R=X/(1-X)$, also holds for the general case. This assumption can be justified by mean-field theory reasoning. In that way, we obtain a general relationship between the diffusion coefficient D^* and the first return probability x. This relation extends the exact result (1.4) for identical scatterers to any mixture of scatterers and also reduces to the RRA in the absence of scatterers. On the other hand, it gives a prediction different from the exact result (1.6) for the deterministic case, although it is still a reasonable approximation. To complete the picture, we need an approximate scheme to obtain x for any given model. This problem was partially addressed in Ref. [11]. Here we extend the mean-field theory developed in Ref. [11] to a hierarchy of systematic approximations.

The paper is organized as follows. The models studied in this paper are described in Sec. II. In Sec. III we make a brief summary of the Boltzmann approximation and the RRA, and propose a new mean-field theory that gives us a relationship between the diffusion coefficient D^* and the first return probability x. This theory is not complete unless we also give an estimate of the first return probability. This is done in Sec. IV, where a sequence of improving mean-field theories for x is derived. The extension of the results of Sec. IV A to the general rotator model and to the mirror model is carried out in Appendix A. The demonstration that $x_B^c=(b-2)/(b-1)$ is the exact percolation threshold for any stochastic model on a lattice of coordination number b is given in Appendix B. The predictions of our mean-field scheme for x and D^* are compared with simulation results in Sec. V. The paper ends with some concluding remarks in Sec. VI.

II. DESCRIPTION OF THE MODELS

A lattice Lorentz gas model is defined by means of two ingredients: the geometry of the substrate lattice and the nature of the scatterers. These scatterers occupy the lattice with a given density ρ, the fraction of scatterers of type a being x_a, so that $\Sigma_a x_a=1$. At this point it is important to note that we are going to discuss only the low-density limit ($\rho\to 0$) of these models. In this situation the particle can return to a previously visited scatterer only with a velocity vector opposite to the initial one, so that it follows trajectories along a Cayley tree. In contrast, when $\rho\neq 0$ there are also polygonal trajectories that contribute to the diffusion coefficient on the same order as those of the Cayley tree. An equivalence can be established between the low-density limit of *stochastic* lattice Lorentz gases defined on a regular lattice with coordination number b and the Cayley tree with the same coordination number. This equivalence is not strictly true in the *deterministic* case because if a particle returns to the origin along a closed loop, it will repeat that loop forever. This means that the polygonal trajectories cannot simply be ignored when the limit $\rho\to 0$ is taken [13]. Nevertheless, we can still define the deterministic Cayley tree model as an independent model, even if it does not adequately represent the low-density limit of the corresponding lattice Lorentz gas.

The collision rules for a given type of scatterer a are defined through a $b\times b$ collision matrix W_a, whose element W_{aij} is the probability that a particle with incident velocity $\mathbf{e}_j$ will be deflected along the direction i. A diagram of the collision rules for right and left rotators on the square lattice is sketched in Fig. 1. Here, the moving particle arrives at the scatterer site from the left. After hitting the right (left) rotator, it has probabilities, α_2, β, α_1, and $\alpha_3=1-\alpha_1-\alpha_2-\beta$ of being transmitted, reflected, deflected to the right (left), and deflected to the left (right), respectively. Pure

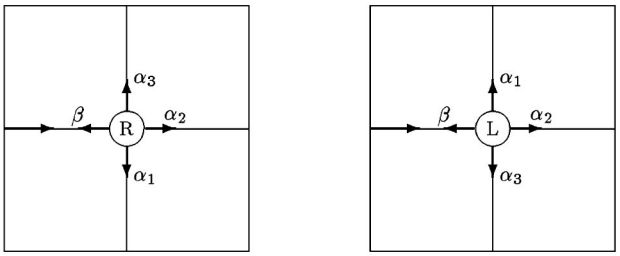

FIG. 1. Right and left rotators on a square lattice. The moving particle enters from the left and collides with the fixed scatterer. The corresponding scattering probabilities are denoted α_1, α_2, α_3, and β.

backscatterers are defined as a special case of rotators with $\beta=1$, $\alpha_1=\alpha_2=\alpha_3=0$. In the rotator model, a fraction x_R (x_L) of the scatterers are right (left) rotators, and a fraction $x_B=1-x_R-x_L$ are pure reflectors. The corresponding collision matrices are

$$W_R=\begin{pmatrix} \alpha_2 & \alpha_1 & \beta & \alpha_3 \\ \alpha_3 & \alpha_2 & \alpha_1 & \beta \\ \beta & \alpha_3 & \alpha_2 & \alpha_1 \\ \alpha_1 & \beta & \alpha_3 & \alpha_2 \end{pmatrix}, \tag{2.1}$$

$$W_L=\begin{pmatrix} \alpha_2 & \alpha_3 & \beta & \alpha_1 \\ \alpha_1 & \alpha_2 & \alpha_3 & \beta \\ \beta & \alpha_1 & \alpha_2 & \alpha_3 \\ \alpha_3 & \beta & \alpha_1 & \alpha_2 \end{pmatrix}, \tag{2.2}$$

$$W_B=\begin{pmatrix} 0 & 0 & 1 & 0 \\ 0 & 0 & 0 & 1 \\ 1 & 0 & 0 & 0 \\ 0 & 1 & 0 & 0 \end{pmatrix}. \tag{2.3}$$

The eigenvalues of these matrices are

$$\omega_{R\ell}=\omega_{L\ell}^*=\alpha_2+\beta(-1)^\ell+\alpha_1 i^\ell+\alpha_3(-i)^\ell, \quad \ell=0,1,2,3, \tag{2.4}$$

$$\omega_{B\ell}=(-1)^\ell, \quad \ell=0,1,\ldots,b-1, \tag{2.5}$$

where i is the imaginary unit. In the deterministic case ($\alpha_1=1$), this model reduces to the one introduced by Gunn and Ortuño [9].

It is straightforward to generalize the rotator model to hexagonal lattices. In that case,

$$W_R=\begin{pmatrix} \alpha_3 & \alpha_2 & \alpha_1 & \beta & \alpha_5 & \alpha_4 \\ \alpha_4 & \alpha_3 & \alpha_2 & \alpha_1 & \beta & \alpha_5 \\ \alpha_5 & \alpha_4 & \alpha_3 & \alpha_2 & \alpha_1 & \beta \\ \beta & \alpha_5 & \alpha_4 & \alpha_3 & \alpha_2 & \alpha_1 \\ \alpha_1 & \beta & \alpha_5 & \alpha_4 & \alpha_3 & \alpha_2 \\ \alpha_2 & \alpha_1 & \beta & \alpha_5 & \alpha_4 & \alpha_3 \end{pmatrix}, \tag{2.6}$$

for right rotators and $W_L=W_R^\dagger$ for left rotators, where the dagger represents the transpose. The eigenvalues are

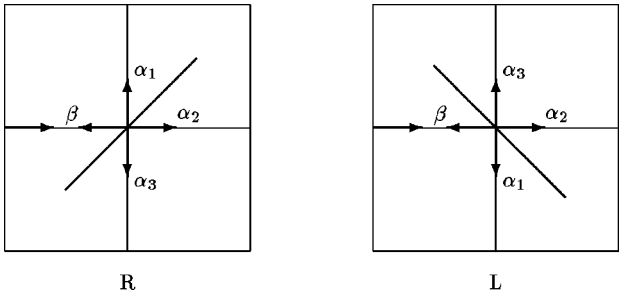

FIG. 2. Same as in Fig. 1 but for right and left mirrors.

$$\omega_{R\ell}=\omega_{L\ell}^*=\alpha_3+\beta(-1)^\ell+[\alpha_2+\alpha_5(-1)^\ell]e^{i\ell\pi/3} +[\alpha_1+\alpha_4(-1)^\ell]e^{i2\ell\pi/3}, \quad \ell=0,\ldots,5. \tag{2.7}$$

In the above rotator models, the relevant eigenvectors for the computation of the diffusion coefficient are $|\varphi_1\rangle=|v_x+iv_y\rangle$ and $|\varphi_{b-1}\rangle=|v_x-iv_y\rangle$, where $|v_\alpha\rangle$, $\alpha=x,y$, is a vector of b components defined as $v_{\alpha i}=e_{i\alpha}$, $i=1,\ldots,b$. Note that the norm is $\langle\varphi_1|\varphi_1\rangle=\langle\varphi_{b-1}|\varphi_{b-1}\rangle=\Sigma_i \mathbf{e}_i\cdot\mathbf{e}_i=b$.

In the rotator model the action of a scatterer is defined with respect to the direction of the moving particle. In the mirror model the action is defined with respect to the orientation of mirrors in the lattice. In this model, there are three types of scatterers on a square lattice: right mirrors, left mirrors, and pure reflectors. The collision rules for right and left mirrors are sketched in Fig. 2. Their collision matrices are

$$W_R=\begin{pmatrix} \alpha_2 & \alpha_1 & \beta & \alpha_3 \\ \alpha_1 & \alpha_2 & \alpha_3 & \beta \\ \beta & \alpha_3 & \alpha_2 & \alpha_1 \\ \alpha_3 & \beta & \alpha_1 & \alpha_2 \end{pmatrix}, \tag{2.8}$$

$$W_L=\begin{pmatrix} \alpha_2 & \alpha_3 & \beta & \alpha_1 \\ \alpha_3 & \alpha_2 & \alpha_1 & \beta \\ \beta & \alpha_1 & \alpha_2 & \alpha_3 \\ \alpha_1 & \beta & \alpha_3 & \alpha_2 \end{pmatrix}, \tag{2.9}$$

with the eigenvalues

$$\omega_{R0}=\omega_{L0}=1, \quad \omega_{R1}=\omega_{L3}=1-2(\beta+\alpha_3), \tag{2.10}$$

$$\omega_{R2}=\omega_{L2}=1-2(\alpha_1+\alpha_3), \quad \omega_{R3}=\omega_{L1}=1-2(\beta+\alpha_1),$$

and relevant eigenvectors $|\varphi_1\rangle=|v_x+v_y\rangle$ and $|\varphi_3\rangle=|v_x-v_y\rangle$. Of course, in stochastic models with $\alpha_1=\alpha_3$, rotators and mirrors become identical scatterers. In the deterministic case ($\alpha_1=1$) and in the absence of pure reflectors ($x_B=0$), the mirror model reduces to the one introduced by Ruijgrok and Cohen [14]. The deterministic mirror model in the presence of backscatterers does not exhibit diffusion, since every trajectory is trapped between two backscatterers with intermediate collisions at the mirrors.

III. DIFFUSION COEFFICIENT

Let us define the one-particle distribution function, $p(\mathbf{n},i,t)$, as the probability that, in a given quenched configuration of scatterers, the particle is at site $\mathbf{n}$ at time t with

a precollisional velocity $\mathbf{e}_i$. This distribution function satisfies a Chapman-Kolmogorov equation

$$p(\mathbf{n}+\mathbf{e}_i,i,t+1)=\left(1-\sum_a c_{a\mathbf{n}}\right)p(\mathbf{n},i,t)+\sum_a c_{a\mathbf{n}}\sum_j W_{aij}p(\mathbf{n},j,t), \quad (3.1)$$

where $c_{a\mathbf{n}}$ is a Boolean variable that takes the value 1 if the site $\mathbf{n}$ is occupied by a scatterer of type a, being 0 otherwise. Obviously, $\langle c_{a\mathbf{n}}\rangle = x_a\rho$, where the angular brackets denote an average over a site-independent distribution of scatterers. In a quenched configuration, the average velocity of the moving particle is $\mathbf{v}(t)=\Sigma_{\mathbf{n}}\Sigma_i p(\mathbf{n},i,t)\mathbf{e}_i$. Thus, the velocity autocorrelation function can be written as

$$\Phi(t)=\Omega\sum_{\mathbf{n}}\sum_{i,j}\mathbf{e}_i\cdot\mathbf{e}_j\langle p(\mathbf{n},i,t)p(\mathbf{0},j,0)\rangle, \quad (3.2)$$

where Ω is the number of sites and we have taken into account the translational invariance property $\langle p(\mathbf{n}+\mathbf{m},i,t)p(\mathbf{n}'+\mathbf{m},j,t')\rangle=\langle p(\mathbf{n},i,t)p(\mathbf{n}',j,t')\rangle$. From the formal solution to Eq. (3.1) and by using standard kinetic theory methods, one can get the following expression for the diffusion coefficient [4,15]:

$$D=\frac{1}{b}\left(\frac{1}{d}\sum_{i,j}\mathbf{e}_i\cdot\mathbf{e}_j\langle\Gamma_{ij}\rangle-1\right), \quad (3.3)$$

where

$$\Gamma=-\frac{1}{\sum_a C_aT_a} \quad (3.4)$$

is the kinetic operator and

$$C_{aij}=c_{a\mathbf{0}}\delta_{ij}, \quad T_{aij}=W_{aij}-\delta_{ij}. \quad (3.5)$$

In the particular case of models on square ($d=2$, $b=4$) or hexagonal ($d=2$, $b=6$) lattices, the general expression for the diffusion coefficient (3.3) in the low-density limit simplifies to [4]

$$D^*=\frac{1}{4}(\lambda_1^{-1}+\lambda_{b-1}^{-1}), \quad (3.6)$$

where λ_1^{-1} and λ_{b-1}^{-1} are the eigenvalues of the operator $\rho\langle\Gamma\rangle$ corresponding to the eigenvectors $|\varphi_1\rangle$ and $|\varphi_{b-1}\rangle$, respectively. In the case of scatterers with rotation symmetry (e.g., rotator model), $\lambda_{b-1}=\lambda_1^*$, while in the case of scatterers with reflection symmetry (e.g., mirror model), both λ_1 and λ_{b-1} are real. In case the system has on average both rotation and reflection symmetries, $\lambda_{b-1}=\lambda_1$.

A. The Boltzmann approximation

This is the simplest mean-field approximation for the calculation of the diffusion coefficient. The Boltzmann approximation is equivalent to assuming that at every time step the configuration of scatterers is chosen randomly among the set of possible configurations. In that way, all the correlations are destroyed and we can write

$$\langle\Gamma\rangle=\left\langle-\frac{1}{\sum_a C_aT_a}\right\rangle\to-\frac{1}{\sum_a\langle C_aT_a\rangle}=-\frac{1}{\rho\sum_a x_aT_a}. \quad (3.7)$$

Consequently, $\lambda_\ell\to 1-\Sigma_a x_a\omega_{a\ell}$, $\ell=0,1,\ldots,b-1$. Making use of Eqs. (2.4), (2.5), (2.7), (2.10), and (3.6), we get

$$D^*=\frac{1}{2}[1-\alpha_2+\beta+x_B(1+\alpha_2-\beta)]^{-1} \quad (3.8)$$

for the rotator and the mirror models on the square lattice and

$$D^*=\frac{1}{2}\left[1-\alpha_3+\beta+\frac{1}{2}(\alpha_1+\alpha_5-\alpha_2-\alpha_4)+x_B\left[1-\beta+\alpha_3+\frac{1}{2}(\alpha_2+\alpha_4-\alpha_1-\alpha_5)\right]\right]^{-1} \quad (3.9)$$

for the hexagonal lattice rotator model. In the above equations we have restricted ourselves to models with equal concentrations of right and left scatterers, i.e., $x_R=x_L=(1-x_B)/2$.

Predictions from Eqs. (3.8) and (3.9) are indeed very poor [12], except for those models where no backscattering is possible ($\beta=0$ and $x_B=0$), in which case no correlated trajectories exist on a Cayley tree. Moreover, the Boltzmann approximation does not predict any percolation threshold in models with pure backscatterers ($x_B\neq 0$). Since the absence of diffusive percolation is a consequence of the trapping of particles in finite clusters surrounded by pure backscatterers, it cannot appear if we do not take into account correlated trajectories.

B. The repeated ring approximation

In order to explain the diffusive behavior of lattice Lorentz gases with a percolation threshold, we need to take into account the correlated sequences of collisions. The simplest sequences of this kind are the so-called ring collisions, in which the particle experiences uncorrelated collisions between successive visits to the same scatterer. First, it is convenient to define the ring operator R so that the element R_{ij} represents the *total* return probability with arrival velocity $\mathbf{e}_i$ at a site visited before, when its departure velocity was $\mathbf{e}_j$. As in the case of the kinetic operator Γ, the ring operator is also defined in a quenched configuration of scatterers. Both fluctuating operators are simply related by [4]

$$R=\frac{1}{\Omega}\sum_{\mathbf{q}}[S(\mathbf{q})-1+\Lambda]^{-1}, \quad (3.10)$$

where $\Lambda\equiv\Gamma^{-1}=-\Sigma_a C_aT_a$ is the collision operator, $S_{ij}(\mathbf{q})=e^{i\mathbf{q}\cdot\mathbf{e}_i}\delta_{ij}$ is the streaming operator in Fourier space, and the $\mathbf{q}$ sum extends over the first Brillouin zone of the reciprocal lattice.

The RRA developed in Ref. [4] is a mean-field theory much more refined than that of the Boltzmann approximation. It consists of replacing the average value $\langle\Gamma\rangle$ in Eq. (3.3) by $\overline{\Lambda}^{-1}$, where $\overline{\Lambda}$ is a nonfluctuating, *effective* collision operator defined in terms of an *effective* ring operator $\overline{R}$ by

$$\overline{\Lambda}=-\rho\sum_a x_a(T_a+T_a\overline{R}T_a+T_a\overline{R}T_a\overline{R}T_a+\cdots)$$

$$=-\rho\sum_a x_a\frac{T_a}{1-\overline{R}T_a}. \tag{3.11}$$

In order to conclude the description, a second condition is needed. In the RRA this is provided by Eq. (3.10) with R and Λ replaced by their effective counterparts, i.e.,

$$\overline{R}=\frac{1}{\Omega}\sum_{\mathbf{q}}[S(\mathbf{q})-1+\overline{\Lambda}]^{-1}. \tag{3.12}$$

Consequently, the eigenvalues λ_ℓ^{-1}, $\ell=0,1,\ldots,b-1$, of $\rho\langle\Gamma\rangle$ are approximated by the reciprocals of the eigenvalues of $\rho^{-1}\overline{\Lambda}$, with the result [4]

$$\lambda_\ell=\sum_a\frac{x_a\tau_{a\ell}}{1+r_\ell\tau_{a\ell}}, \tag{3.13}$$

$$r_\ell=\begin{cases}-\frac{1}{2}+\frac{1}{2}z, & \ell=\text{even}\\ -\frac{1}{2}+\frac{1}{2}z^{-1}, & \ell=\text{odd}\end{cases} \tag{3.14}$$

where $\tau_{a\ell}\equiv1-\omega_{a\ell}$ are the eigenvalues of $-T_a$, r_ℓ are the eigenvalues of $\overline{R}$, and z is a parameter that verifies the algebraic equation

$$\sum_a x_a\left[z\sum_{\ell\neq0}^{(+)}\frac{\tau_{a\ell}}{2+(z-1)\tau_{a\ell}}-z^{-1}\sum_{\ell}^{(-)}\frac{\tau_{a\ell}}{2+(z^{-1}-1)\tau_{a\ell}}\right]=0, \tag{3.15}$$

where the subscripts denote a summation over even $(+)$ or odd $(-)$ ℓ values only. Upon deriving Eqs. (3.14) and (3.15), the low-density limit $\rho\to0$ and the thermodynamic limit $\Omega\to\infty$ have already been taken. It is interesting to note that in the case of the models introduced in Sec. II, the parameter z does not explicitly depend on the fraction of right or left scatterers, but only on the concentration of pure backscatterers, x_B.

The RRA reduces to the exact result of van Beijeren and Ernst in the case of identical scatterers [4,7] and is also exact for mixtures of symmetric scatterers without pure backscatterers, according to comparison with simulation results [12]. On the other hand, its predictions are very poor for any model including backscatterers ($x_B\neq0$). As said before, in these models the backscatterers act as obstacles to particle diffusion so that if x_B is larger than a threshold value x_B^c the diffusion coefficient vanishes. While the RRA succeeds in predicting the existence of this percolation threshold, which is associated with the root $z\to\infty$ in Eq. (3.15), it gives a bad estimate for its numerical value, namely, $x_B^c=(b-2)/2(b-1)$, which is half the value obtained by means of simple arguments of percolation theory [10].

For the sake of illustration, we give below the RRA predictions in some representative cases. In the deterministic rotator model ($\alpha_1=1$, $\alpha_2=\alpha_3=\beta=0$), one has

$$D^*=\frac{1}{2(1-x_B)}\sqrt{\frac{1-3x_B}{1+x_B}}. \tag{3.16}$$

For the model of isotropic scatterers both in square and hexagonal lattices ($\alpha_1=\cdots=\alpha_{b-1}=\beta=b^{-1}$),

$$D^*=\frac{b-1}{2b}\left[1-\frac{2(b-1)}{b-2}x_B\right]. \tag{3.17}$$

For the forward isotropic model ($\alpha_1=\alpha_2=\alpha_3=\frac{1}{3}$, $\beta=0$),

$$D^*=\frac{3}{4}(1-3x_B). \tag{3.18}$$

Finally, in the case of the quasi-isotropic mirror model ($\alpha_1=\alpha_2=\beta=\frac{1}{3}$, $\alpha_3=0$),

$$D^*=\frac{2z^2+5z+2}{2z(4+5z)(1+zx_B)},$$

$$z=\frac{2+3x_B+\sqrt{9x_B^2-12x_B+12}}{2(1-3x_B)}. \tag{3.19}$$

These examples show that $D^*\to0$ as $x_B\to(b-2)/2(b-1)$. The predicted value of the critical exponent defined in (1.8) is $\mu=1$ for the stochastic models and $\mu=\frac{1}{2}$ for the deterministic rotator model. Note that in the latter model the exact value is $\mu=2$.

C. An alternative mean-field approximation

The poor predictions of the RRA in models with a percolation threshold can be traced back to Eq. (3.12), where the effective ring operator is connected to the effective collision operator through the same relation that holds between the corresponding fluctuating operators, Eq. (3.10). From Eqs. (2.5), (3.13), and (3.14), we can see that the contribution to λ_1 and λ_{b-1} associated with the pure backscatterers is $2zx_B$. In the vicinity of the fraction $x_B=(b-2)/2(b-1)$, Eq. (3.15) yields $z\sim[(b-2)/2(b-1)-x_B]^{-1}$, $\ell=1,2,\ldots,b-1$ so that the diffusion coefficient given by Eq. (3.6) vanishes at the RRA percolation threshold $x_B^c=(b-2)/2(b-1)$. Thus, we conclude that this wrong value of x_B^c is built into Eq. (3.12) or, equivalently, Eq. (3.15).

In order to overcome the above difficulty, we propose here a mean-field approach different from that of the previous subsection. In this new approach, the relationship (3.11) between the effective operators $\overline{\Lambda}$ and $\overline{R}$ is kept. Nevertheless, instead of using Eq. (3.12), we express the ring operator $\overline{R}$ as

$$\overline{R}=X+X^2+X^3+\cdots=\frac{X}{1-X}, \tag{3.20}$$

where X_{ij} is the (effective) *first* return probability with velocity $\mathbf{e}_i$ to a given site that was left by the particle with velocity $\mathbf{e}_j$. In the particular case of Cayley trees, only those elements of X with indices i and j corresponding to opposite directions are nonzero, $X_{ij}=x\delta_{i,j\pm b/2}$, where x is the first return probability summed over all possible initial and final velocities. As a consequence, the eigenvalues of $\overline{R}$ are

$$r_\ell=\frac{(-1)^\ell x}{1-(-1)^\ell x}, \quad \ell=0,1,\ldots,b-1. \tag{3.21}$$

Note that Eq. (3.21) is equivalent to Eq. (3.14) if the parameter z is identified as

$$z=\frac{1+x}{1-x}. \tag{3.22}$$

Thus, the mean-field approximation developed in this paper differs from the RRA only in the fact that, instead of using Eq. (3.15), the first return probability x will be obtained by independent reasoning.

The meaning of Eq. (3.20) is clear. The total return probability is expressed as the sum of the first return probability, the second return probability, and so on, where the nth return probability is assumed to be the first return probability raised to the nth power. This implies the absence of correlations between the returning probabilities along all the particle trajectories. This assumption is not correct in general, but it yields good results, as will be shown later. Moreover, if all the scatterers are identical, then the same first return probability can be assigned to every trajectory, since this quantity is independent of the specific form of the path and only depends on the scattering rules of the scatterers that the particle finds along its path. So, Eq. (3.20) is exact for the case of identical scatterers. As a matter of fact, relations (3.20) and (3.22) were already found in Ref. [4] in connection with the identical scatterer limit of the RRA. Since we know that the RRA gives the exact diffusion coefficient in this limit, the theory proposed here will also be exact in that case. An analogous situation takes place in models without backscatterers. If all the scatterers are right or left rotators (or mirrors), the set of scattering probabilities is the same for both species, except for a symmetry rule. This means that the first return probability is also independent of the specific configuration in this case, so that it is independent of the fraction of right (or left) scatterers. This property is also verified by z in Eq. (3.15) and Eq. (3.22) also holds for mixtures of symmetric scatterers. Thus, the predictions of the RRA and the theory presented here coincide in this case with $x_B=0$.

To be more specific, let us write down the relationship between the reduced diffusion coefficient, Eq. (3.6), and the first return probability for the same examples as in the preceding subsection. The results are

$$D^*=\frac{1-x}{2(1+x)}\,\frac{1+x^2}{(1+x^2)(1+x_B)-2x(1-x_B)}, \tag{3.23}$$

$$D^*=\frac{1-x}{2(1+x)}\,\frac{1}{1+x_B-x(1-x_B)}, \tag{3.24}$$

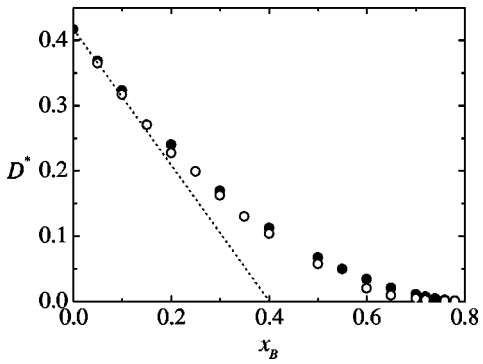

FIG. 3. Diffusion coefficient for the isotropic model on the hexagonal lattice ($\alpha_1=\cdots=\alpha_5=\beta=\frac{1}{6}$). The Monte Carlo data points are denoted by open circles. The dotted line corresponds to the repeated ring approximation and the closed circles are obtained from the mean-field theory relation between D^* and x, Eq. (3.24), by using the simulation results of x as input.

$$D^*=\frac{1-x}{4(1+x)}\,\frac{3+x}{1+2x_B-x(1-2x_B)}, \tag{3.25}$$

$$D^*=\frac{1-x}{2(1+x)}\,\frac{9-x^2}{(9+x)[1+x_B-x(1-x_B)]}, \tag{3.26}$$

for the deterministic rotator model ($\alpha_1=1$, $\alpha_2=\alpha_3=\beta=0$), the model of isotropic scatterers on both square and hexagonal lattices ($\alpha_1=\cdots=\alpha_{b-1}=\beta=b^{-1}$), the forward isotropic model ($\alpha_1=\alpha_2=\alpha_3=\frac{1}{3}$, $\beta=0$), and the quasi-isotropic mirror model ($\alpha_1=\alpha_2=\beta=\frac{1}{3}$, $\alpha_3=0$), respectively. It is important to remark that the mean-field prediction (3.23) differs from the low-density limit of the exact result (1.6). Nevertheless, the relative error of Eq. (3.23) is less than 4% in the interval $0\leqslant x_B<0.6$. The relative error increases near the percolation threshold since Eq. (3.23) predicts that D^* vanishes with a critical exponent $\mu=1$, while the exact value is $\mu=2$.

The mean-field approximation characterized by Eqs. (3.11) and (3.20) or, equivalently, Eqs. (3.13) and (3.21) is not complete unless we propose an approximate scheme to obtain the first return probability x for a given model. This is done in Sec. IV, where a renormalizable mean-field theory for the calculation of x is developed. Before that, however, it is instructive to compare simulation results of D^* (see Sec. V) with those obtained from Eqs. (3.6), (3.13), and (3.21), by using the corresponding *simulation* results for x. Figure 3 shows such a comparison in the case of a model of isotropic scatterers ($\alpha_1=\cdots=\alpha_5=\beta=\frac{1}{6}$) plus backscatterers on the hexagonal lattice. The RRA predictions are also shown. For $x_B\leqslant 0.1$ both theories agree well with the simulation results. For larger concentrations of backscatterers, however, the RRA rapidly deviates from the simulation results, while our approximation exhibits quite good agreement. On the other hand, we must emphasize that the mean-field approximation represented by the closed circles in Fig. 3 is still semi-empirical, since the simulation results for x have been used as input. The self-contained approximation constructed from the theoretical analysis of Sec. IV will be compared with simulations in Sec. V.

IV. FIRST RETURN PROBABILITY

The first return probability on a *deterministic* Cayley tree with rotators and backscatterers defined on a lattice with coordination number b is simply given by the root of

$$x = x_B + (1-x_B)x^{b-1}, \tag{4.1}$$

which is a straightforward generalization of Eq. (1.7). Equation (4.1) means that there are two excluding possibilities for the return of the particle to the origin: either (i) the first scatterer found is a backscatterer, so that it returns for sure, or (ii) the first scatterer visited is a rotator and then the particle has to visit the other $b-1$ branches of the Cayley tree starting from the rotator in strict order until it finally returns to the origin, which happens with probability x^{b-1}. The first event has a probability x_B, while the probability of the second event is $1-x_B$. By differentiating both sides of Eq. (4.1) with respect to x and then making $x=1$ we obtain the percolation threshold $x_B^c=(b-2)/(b-1)$. The situation in stochastic models is more complicated, since the moving particle can visit the same branch of the Cayley tree many times before returning to the origin. A simple mean-field approach to this problem was given in Ref. [11]. Here, we extend that result and present a set of generalized mean-field theories that give better and better predictions as larger and larger clusters of the Cayley tree around the origin are averaged exactly. For the sake of clarity, we consider in this section the case of the rotator model on the square lattice only. Extension of these results to the mirror model and to the hexagonal lattice (or lattices with a higher coordination number) are straightforward and given in Appendix A.

A. First return probability in a quenched configuration

Consider now the function $f(x_1,x_2,x_3)$ defined as the probability of the first return to the origin, in a *quenched* configuration, provided that the first scatterer visited by the moving particle is a right rotator (R) and that the return probabilities to that scatterer along the remaining three branches of the Cayley tree are x_1, x_2, and x_3 (in counterclockwise order). This function can be written as the following sum:

$$f(x_1,x_2,x_3) = \sum_{n=0}^{\infty} \gamma_n(x_1,x_2,x_3), \tag{4.2}$$

where $\gamma_n(x_1,x_2,x_3)$, $n=0,1,2,\ldots$, is the first return probability after $n+1$ visits to R. A simple path counting yields

$$\gamma_0 = \beta, \tag{4.3a}$$

$$\gamma_1 = \alpha_1 x_1 \alpha_3 + \alpha_2 x_2 \alpha_2 + \alpha_3 x_3 \alpha_1, \tag{4.3b}$$

$$\begin{aligned}\gamma_2 = {} & \alpha_1 x_1 (\beta x_1 \alpha_3 + \alpha_1 x_2 \alpha_2 + \alpha_2 x_3 \alpha_1) \\ & + \alpha_2 x_2 (\alpha_3 x_1 \alpha_3 + \beta x_2 \alpha_2 + \alpha_1 x_3 \alpha_1) \\ & + \alpha_3 x_3 (\alpha_2 x_1 \alpha_3 + \alpha_3 x_2 \alpha_2 + \beta x_3 \alpha_1).\end{aligned} \tag{4.3c}$$

Thus, γ_0 corresponds to a particle which after colliding with R is directly backscattered. The probability of first return after two previous visits to R, γ_1, is written as the sum of three terms: the first (third) term corresponds to a particle that is deflected to the right (left), returns to R, and then is deflected to the left (right), so that it finally returns to the origin; the second term corresponds to a particle that, after being transmitted, returns to R and is again transmitted. Equation (4.3c) can be explained in a similar way. The explicit relations (4.3) are sufficient to convince oneself that the general relation can be written as

$$\gamma_n(x_1,x_2,x_3) = \boldsymbol{\alpha}^\dagger \cdot \boldsymbol{\zeta}_n(x_1,x_2,x_3), \tag{4.4}$$

where

$$\boldsymbol{\alpha} = \begin{pmatrix} \alpha_1 \\ \alpha_2 \\ \alpha_3 \end{pmatrix} \tag{4.5}$$

and $\boldsymbol{\zeta}_n(x_1,x_2,x_3)$ satisfies the following recurrence relation:

$$\boldsymbol{\zeta}_{n+1} = \mathsf{X}\cdot\mathsf{M}\cdot\boldsymbol{\zeta}_n = (\mathsf{X}\cdot\mathsf{M})^n \cdot \mathsf{X}\cdot\boldsymbol{\alpha}', \tag{4.6}$$

with

$$\mathsf{X} = \begin{pmatrix} x_1 & 0 & 0 \\ 0 & x_2 & 0 \\ 0 & 0 & x_3 \end{pmatrix}, \quad \mathsf{M} = \begin{pmatrix} \beta & \alpha_1 & \alpha_2 \\ \alpha_3 & \beta & \alpha_1 \\ \alpha_2 & \alpha_3 & \beta \end{pmatrix},$$

$$\boldsymbol{\alpha}' = \begin{pmatrix} \alpha_3 \\ \alpha_2 \\ \alpha_1 \end{pmatrix}. \tag{4.7}$$

From Eqs. (4.2), (4.4), and (4.6), we have

$$\begin{aligned} f(x_1,x_2,x_3) &= \beta + \sum_{n=1}^{\infty} \boldsymbol{\alpha}^\dagger \cdot (\mathsf{X}\cdot\mathsf{M})^{n-1} \cdot \mathsf{X}\cdot\boldsymbol{\alpha}' \\ &= \beta + \boldsymbol{\alpha}^\dagger \cdot (1-\mathsf{X}\cdot\mathsf{M})^{-1} \cdot \mathsf{X}\cdot\boldsymbol{\alpha}'. \end{aligned} \tag{4.8}$$

Inserting Eqs. (4.5) and (4.7) into Eq. (4.8), we explicitly get

$$f(x_1,x_2,x_3) = \beta + \frac{g(x_1,x_2,x_3)}{\Delta(x_1,x_2,x_3)}, \tag{4.9}$$

where

$$g(x_1,x_2,x_3)=\alpha_1\alpha_3x_1(1-\beta x_2)(1-\beta x_3)+\alpha_2^2x_2(1-\beta x_1)(1-\beta x_3)+\alpha_1\alpha_3x_3(1-\beta x_1)(1-\beta x_2)+\alpha_2(\alpha_1^2+\alpha_3^2)$$
$$\times[(1-\beta x_3)x_1x_2+(1-\beta x_2)x_1x_3+(1-\beta x_1)x_2x_3]+[(\alpha_1^2-\alpha_3^2)^2+\alpha_2^2(4\alpha_1\alpha_3-\alpha_2^2)]x_1x_2x_3 \quad (4.10)$$

and

$$\Delta(x_1,x_2,x_3)=(1-\beta x_1)(1-\beta x_2)(1-\beta x_3)-\alpha_2(\alpha_1^2+\alpha_3^2)x_1x_2x_3-\alpha_2^2x_1x_3(1-\beta x_2)-\alpha_1\alpha_3x_2x_3(1-\beta x_1)$$
$$-\alpha_1\alpha_3x_1x_2(1-\beta x_3) \quad (4.11)$$

is the determinant of $\mathsf{X}\cdot\mathsf{M}$.

As a simple test of consistency, notice that $f(1,1,1)=1$, i.e., if the particle always returns to R along any of the three outgoing branches, then the probability of returning to the origin is 1. The general expression (4.9) simplifies in some interesting cases. For instance, in the particular case of isotropic scatterers ($\alpha_1=\alpha_2=\alpha_3=\beta=\frac{1}{4}$), one easily gets

$$f(x_1,x_2,x_3)=\frac{1}{4-x_1-x_2-x_3}. \quad (4.12)$$

In the case of forward isotropic scatterers ($\alpha_1=\alpha_2=\alpha_3=\frac{1}{3}$, $\beta=0$), Eq. (4.9) becomes

$$f(x_1,x_2,x_3)=\frac{3(x_1+x_2+x_3)+2(x_1x_2+x_1x_3+x_2x_3)+x_1x_2x_3}{27-3(x_1x_2+x_1x_3+x_2x_3)-2x_1x_2x_3}. \quad (4.13)$$

As a third example, let us consider the deterministic rotator model ($\alpha_1=1$, $\alpha_2=\alpha_3=\beta=0$), in which case $f(x_1,x_2,x_3)=x_1x_2x_3$.

The function $f(x_1,x_2,x_3)$ corresponding to those trajectories with a left rotator (L) as the first scatterer found is the same for these models as the one corresponding to R, provided that the branches with return probabilities x_1, x_2, and x_3 are now considered in clockwise order.

B. Average first return probability

From the definition of $f(x_1,x_2,x_3)$ it is obvious that the (average) first return probability satisfies the following equation:

$$x=x_B+(1-x_B)\langle f(x_1,x_2,x_3)\rangle, \quad (4.14)$$

where the brackets denote an average over all possible configurations. Indefinitely ramified Cayley trees are included in this average, so that it is not possible to compute it exactly. Obviously, $\langle x_1\rangle=\langle x_2\rangle=\langle x_3\rangle=x$. On the other hand, although x_1, x_2, and x_3 are statistically independent, i.e., $\langle x_1^{n_1}x_2^{n_2}x_3^{n_3}\rangle=\langle x_1^{n_1}\rangle\langle x_2^{n_2}\rangle\langle x_3^{n_3}\rangle$, one has $\langle x_1^{n_1}\rangle\neq x^{n_1}$, $n_1>1$. The simplest mean-field approximation is obtained by substituting every branch of the Cayley tree starting from the first scatterer visited by an average branch with an average return probability. In this approximation, $\langle f(x_1,x_2,x_3)\rangle \rightarrow f(\langle x_1\rangle,\langle x_2\rangle,\langle x_3\rangle)=f(x,x,x)$ and Eq. (4.14) becomes

$$x=x_B+(1-x_B)f(x,x,x). \quad (4.15)$$

The mean-field theory (4.15), which we will refer to as the zeroth-order approximation to Eq. (4.14), was formulated and analyzed in Ref. [11]. An improved (i.e., first-order) mean-field theory is obtained if we explicitly include in the configurational average the nearest neighbors on the Cayley tree of the first scatterer visited. If the nearest neighbor of the initial rotator along a given path is a backscatterer, then the return probability along that path will be taken as 1; in the case where one of the nearest neighbors of the first scatterer visited is a rotator, the probability of return along that path will be assumed to be

$$y=\frac{x-x_B}{1-x_B}. \quad (4.16)$$

An average over all the possible configurations of the nearest neighbors of the first rotator visited by the moving particle yields the following equation for x:

$$x=x_B+(1-x_B)\{x_B^3f(1,1,1)+(1-x_B)^3f(y,y,y)$$
$$+x_B^2(1-x_B)[f(1,1,y)+f(1,y,1)+f(y,1,1)]$$
$$+x_B(1-x_B)^2[f(1,y,y)+f(y,1,y)+f(y,y,1)]\}. \quad (4.17)$$

The meaning of Eq. (4.17) is clear; the first term on the right-hand side corresponds to the collision of the moving particle with a backscatterer after leaving the origin; the second term corresponds to those trajectories where the particle collides first with a rotator and then encounters three backscatterers on the branches of the tree, so that the particle returns to the origin with probability $f(1,1,1)=1$; the third term corresponds to the case where the first scatterer is a rotator and its nearest neighbors are also rotators. The other terms have similar interpretations. Inserting Eq. (4.16) into Eq. (4.17), we get a closed equation for x whose solution is expected to be a better estimate of the first return probability than the solution of Eq. (4.15).

More generally, we can write the nth-order approximation in the form

$$x=x_B+(1-x_B)\sum_{\mathcal{C}_n}\mathcal{P}(\mathcal{C}_n)f_{\mathcal{C}_n}(y), \quad (4.18)$$

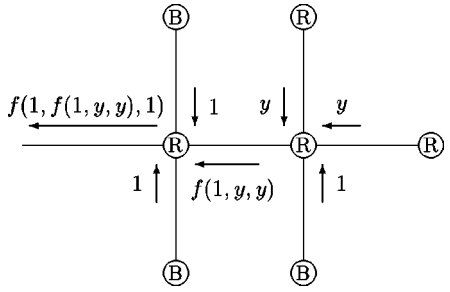

FIG. 4. A typical configuration of a Cayley tree to generation $n=2$. The corresponding probability of first return to the origin is $f(1,f(1,y,y),1)$, where y is the first return probability on the assumption that the first scatterer visited is a rotator.

where the sum runs over all possible configurations $\{\mathcal{C}_n\}$ that include the nth-order neighbors of the first rotator found, $\mathcal{P}(\mathcal{C}_n)$ is the probability of that configuration, and $f_{\mathcal{C}_n}(y)$ is the corresponding first return probability. Of course, $\Sigma_{\mathcal{C}_n}\mathcal{P}(\mathcal{C}_n)=1$. For example, Fig. 4 shows a typical configuration corresponding to $n=2$. The probability of that configuration is $\mathcal{P}(\mathcal{C}_2)=x_B^3(1-x_B)^3$ and $f_{\mathcal{C}_2}(y)=f(1,f(1,y,y),1)$. An example of third-order configuration can be obtained from the second-order configuration of Fig. 4 by assuming that the two outermost rotators are surrounded, for instance, by three rotators and by one rotator and two backscatterers, respectively. In that case, $\mathcal{P}(\mathcal{C}_3)=x_B^5(1-x_B)^7$ and $f_{\mathcal{C}_3}(y)=f(1,f(1,f(y,y,y),f(y,1,1)),1)$. In general, $f_{\mathcal{C}_n}(y)$ can include up to n levels of nested f functions. The number of terms on the right-hand side of Eq. (4.18) increases with n faster than exponentially. In a Cayley tree of coordination number equal to b, the number $\mathcal{N}_n$ of different configurations involving up to the nth generation of neighbors satisfies the recurrence relation $\mathcal{N}_n=\Sigma_{m=0}^{b-1}\binom{b-1}{m}\mathcal{N}_{n-1}^m=(1+\mathcal{N}_{n-1})^{b-1}$, with $\mathcal{N}_1=2^{b-1}$, so that $\log\mathcal{N}_n\simeq\text{const}\times(b-1)^n$. Even when the number of configurations essentially different can be reduced if the rotators are sufficiently symmetric, only the theories of the lowest orders are manageable. In the next section we compare the predictions for $n=0,1,2$ with Monte Carlo simulation results for some models.

The renormalization scheme outlined in this section is still useful to obtain some important properties of the first return probability, such as the percolation threshold. In Appendix B it is shown that the percolation threshold x_B^c is a fixed point of the renormalization transformation and takes the value $x_B^c=(b-2)/(b-1)$ for all models defined on a lattice of cordination number b. It is also proved there that in the critical region [cf. Eq. (B14)]

$$1-x\approx A_n(x_B^c-x_B),\quad A_n^{-1}\equiv\frac{1}{2n}\frac{\partial^2 h_n}{\partial y^2}\bigg|_{x_B=x_B^c,y=1},\quad n\geq 1, \tag{4.19}$$

where $h_n(y,x_B)$ is given by Eq. (B7). This implies that $D^*\sim x_B^c-x_B$ (i.e. $\mu=1$) in our mean-field theory, as seen, for instance, from Eqs. (3.23)–(3.26).

As shown in Appendix B, Eq. (4.18) gives the exact first return probability, regardless of the order n of the approximation, in three special cases: the deterministic rotator (or Gunn-Ortuño) model, the deterministic mirror (or Ruijgrok-Cohen) model, and stochastic models in the absence of backscatterers. In the latter case, moreover, the theory developed in this section coincides with the RRA.

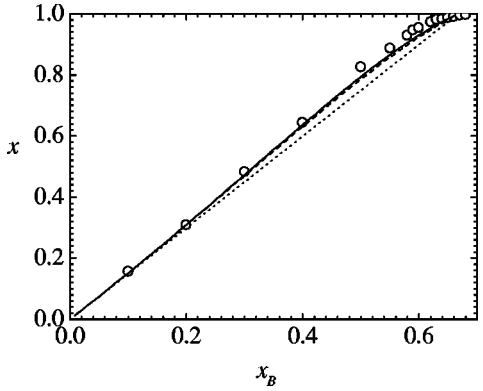

FIG. 5. First return probability for the forward isotropic model on the square lattice ($\alpha_1=\alpha_2=\alpha_3=\frac{1}{3}$, $\beta=0$). The Monte Carlo data points are denoted by open circles. The dotted line, broken line, and solid line correspond to the predictions of the mean-field theory of orders $n=0$, $n=1$, and $n=2$, respectively.

V. COMPARISON WITH MONTE CARLO SIMULATIONS

In order to test the reliability of the theories developed in Secs. III and IV, the diffusion coefficient and the first return probability have been measured by means of Monte Carlo simulations performed on Cayley trees. We have used the Cayley tree method discussed in Refs. [11] and [12]. Rather than performing simulations on a regular lattice for finite ρ and then taking the limit $\rho\to 0$, we have directly worked in that limit by considering the scaled distance $\mathbf{r}^*=\rho\mathbf{r}$ and time $t^*=\rho t$, which become continuous variables in the limit $\rho\to 0$. In the method we used, the scatterers already visited by the moving particle are labeled and a matrix is used to store the labels of the nearest neighbors of every scatterer placed in the tree. If the particle is deflected along a path occupied by a scatterer, the above matrix gives information on the type of the scatterer to be found and on its distance from the previous scatterer. In the case where the particle is deflected along a branch not previously explored, a new scatterer of type a is placed with a probability equal to x_a and at a distance r^* drawn from the Poisson distribution $P(r^*)=e^{-r^*}$. Thus, the Cayley tree grows as the particle moves, so that the averages over configurations and trajectories are computed simultaneously. We have evaluated the velocity autocorrelation function $\Phi(t^*)$ at $t^*=\Delta t^*,2\Delta t^*,\ldots$, by averaging the dot product $\mathbf{v}(0)\cdot\mathbf{v}(t^*)$ over a large number N of trajectories. Then the reduced diffusion coefficient D^* is numerically evaluated from the Green-Kubo formula

$$D^*=\lim_{t^*\to\infty}\frac{1}{d}\int_0^{t^*}d\tau\Phi(\tau)\simeq\frac{1}{d}\int_0^{t^*_{\max}}d\tau\Phi(\tau). \tag{5.1}$$

In the region $x_B\leq 0.5$ we have typically taken $\Delta t^*=0.1$ and $N=2\times 10^5$, and the maximum simulation time was about $t^*_{\max}=25$. On the other hand, the diffusion coefficient is too

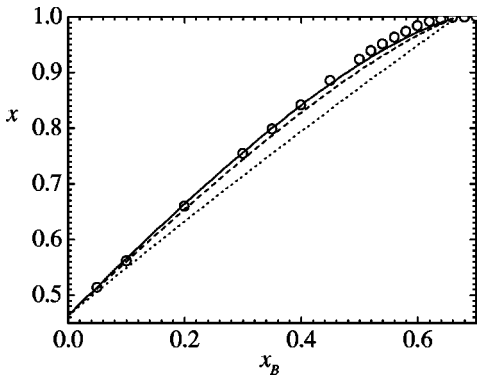

FIG. 6. Same as in Fig. 5 but for the quasi-isotropic mirror model ($\alpha_1=\alpha_2=\beta=\frac{1}{3},\ \alpha_3=0$).

small for $x_B \geqslant 0.5$, so that a larger number of trajectories and larger simulation times are required to get accurate values; in this region we have used $N=10^8$ trajectories until a maximum time $t^*_{\max}=10^4$. The first return probability x is approximately computed in the simulations as the fraction of particles that return for the first time to the starting site before a given time t_0^* much larger than the average return time. Usually, $t_0^*=1500$ is sufficient, except for x_B very close to x_B^c [11]. Although this method always provides a lower bound to the correct first return probability, the fraction of returning particles not accounted for is exponentially small.

A comparison between the Monte Carlo simulation results for x and the predictions of the mean-field theories discussed in the preceding section is performed in Figs. 5 and 6 for the square-lattice models of forward isotropic scatterers and quasi-isotropic mirrors, respectively. In these figures, the dotted lines correspond to the zeroth-order mean-field theory, the broken lines to the first-order mean-field theory, and the solid lines to the second-order theory. The first-order theory improves significantly the predictions of the zeroth-order theory already presented in Ref. [11]. The subsequent improvement of the second-order approximation is still noticeable but less dramatic. In general, the convergence of the nth-order approximation, Eq. (4.18), towards the exact result as $n\to\infty$ is expected to be very slow, so that $n=2$ gives an optimal compromise between simplicity and reliability. We have checked that a behavior similar to that of Figs. 5 and 6 is found for the model of isotropic scatterers on square or hexagonal lattices. In the latter case, since the coordination number is larger than in the case of a square lattice and correlations become less likely, the theory with $n=1$ is seen to be sufficient. It is worth remarking that the agreement between the mean-field theories and the Monte Carlo results worsens, as expected, near the percolation threshold. While the theories with finite n predict that $1-x \sim x_B^c - x_B$ [cf. Eq. (4.19)], the simulation results seem to indicate a critical exponent larger than 1. Thus we speculate that the amplitude A_n in (4.19) goes to 0 as $n\to\infty$.

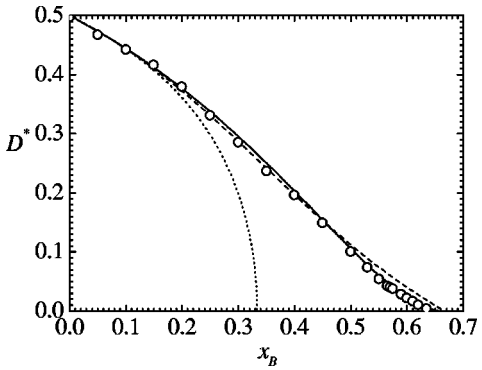

FIG. 7. Diffusion coefficient for the deterministic rotator model on the square lattice ($\alpha_1=1,\ \alpha_2=\alpha_3=\beta=0$). The Monte Carlo data points are shown as open circles. The dotted line is the prediction of the repeated ring approximation, the broken line corresponds to the mean-field theory discussed in this paper, and the solid line is the exact result.

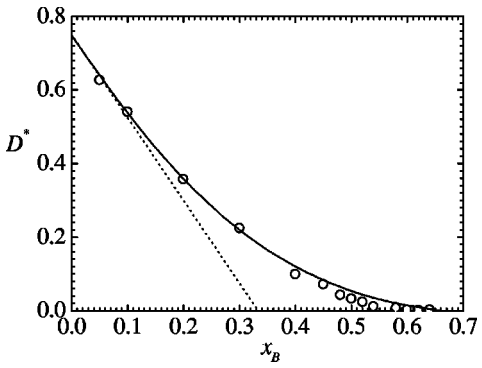

FIG. 8. Diffusion coefficient for the forward isotropic model defined on the square lattice ($\alpha_1=\alpha_2=\alpha_3=\frac{1}{3},\ \beta=0$). The repeated ring approximation prediction is shown as a dotted line, the theory presented in this paper corresponds to the solid line, and the open circles are the results of the Monte Carlo simulation.

Let us now consider the behavior of the diffusion coefficient. In Fig. 7 the simulation results of D^* for the *deterministic* rotator model are compared with the exact result, Eq. (1.6), the RRA prediction, Eq. (3.16), and our mean-field theory, Eq. (3.23). While the original RRA can be trusted for $x_B \leqslant 0.2$ only, our alternative mean-field theory is reliable in the range $x_B \leqslant 0.5$; for greater concentrations of backscatterers the predicted diffusion coefficient is too large as compared with the exact result. There is no exact result for the diffusion coefficient on *stochastic* Cayley trees. Thus it is indeed rewarding to realize that the mean-field theory we have proposed in this paper provides a good estimate in all the cases studied. This is illustrated in Figs. 8 and 9 for the forward isotropic model and the quasi-isotropic mirror

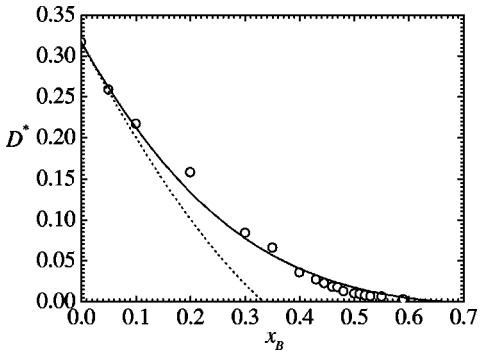

FIG. 9. Same as in Fig. 8 but for the quasi-isotropic mirror model ($\alpha_1=\alpha_2=\beta=\frac{1}{3},\ \alpha_3=0$).

model, respectively. The RRA predictions (dotted lines) are given by Eqs. (3.18) and (3.19); the solid lines correspond to Eqs. (3.25) and (3.26), supplemented by the second-order mean-field theory to determine x, although the use of the zeroth-order theory, Eq. (4.15), already yields fairly good results. As expected, the agreement between the simulation results and the theory developed in this paper becomes worse near the percolation threshold. In fact, our mean-field approximation predicts that the critical exponent defined in Eq. (1.8) is $\mu=1$, while the simulation data support the value $\mu\simeq 2$.

VI. CONCLUDING REMARKS

In this paper we have proposed a mean-field theory for the diffusion coefficient of a particle moving on a Cayley tree, whose sites are occupied by scatterers of several types, including a fraction x_B of backscatterers. These backscatterers block the growth of the tree and are responsible for the absence of percolation and diffusion if their concentration exceeds a certain critical value x_B^c. The Cayley tree corresponds to the low-density limit of lattice Lorentz gases with pointlike scatterers, except for the deterministic case [13]. The theory is built upon three independent mean-field assumptions: (a) the relationship (3.11) between an effective collision operator $\overline{\Lambda}$ and an effective ring operator $\overline{R}$, which takes into account the so-called repeated ring collisions; (b) the relationship (3.20) between the ring operator and the first return probability matrix X; and (c) a hierarchy of mean-field theories for the first return probability x discussed in Sec. V. In the repeated ring approximation, on the other hand, assumptions (b) and (c) are replaced by the self-consistency condition (3.12). While both theories are equivalent in the absence of backscatterers ($x_B=0$, in which case they give the exact diffusion coefficient), they strongly deviate from each other as x_B increases. In fact, the RRA predicts that the diffusion coefficient vanishes for x_B equal to or larger than $(b-2)/2(b-1)$, where b is the coordination number, which is half the value of the correct percolation threshold $x_B^c=(b-2)/(b-1)$ predicted by our theory. Comparison with Monte Carlo simulations for several models of rotators or mirrors with backscatterers has shown that the theory presented in this paper gives a very good approximation to the first return probability and the diffusion coefficient. An interesting conclusion of the theory is that the diffusive percolation threshold (fraction of backscatterers beyond which the diffusion coefficient vanishes) coincides with the percolation threshold (fraction of backscatterers beyond which the first return probability becomes 1), and that this value depends only on the coordination number of the lattice and not on the collision rules for the scatterers included in the model. These predictions are confirmed by simulations.

It is interesting to point out that in the three mean-field approaches considered in this paper the diffusion coefficient is given by Eqs. (3.6), (3.13), and (3.14). The differences are that in the Boltzmann approximation $z=1$ (which implies $x=0$), in the RRA z is the root of Eq. (3.15), while in our theory $z=(1+x)/(1-x)$ with x being the root of Eq. (4.15), (4.17), or, more generally, Eq. (4.18). The three theories are identical when no retracing trajectories are possible ($\beta=0$ and $x_B=0$, so that $x=0$), the two latter theories coincide if backscatterers are absent ($x_B=0$), and only our theory remains reliable whenever a percolation threshold exists ($x_B\neq 0$).

The mean-field theory proposed in this paper could be improved along several directions. First, the repeated ring expression for the collision operator, Eq. (3.11), could be extended to take into account nonring collisions, such as nested rings. Moreover, the purely mean-field ring operator in Eq. (3.20) could be modified to consider correlations between successive visits of the particle to the same branches of the tree. As for the determination of x, although the scheme outlined in Sec. V admits in principle its systematic implementation to higher and higher orders, this is in practice hindered by the rapid increase of the associated algebraic complexity. Since we have used here the second-order approximation for x, we can say that it implies a higher degree of refinement than that of Eqs. (3.11) and (3.20). In this respect, it is worth noting that even when using the zeroth-order approximation (4.15) one obtains fairly good estimates, the resulting theory having the same degree of algebraic complexity as in the RRA. Finally, it is tempting to speculate that the methods proposed in this paper might have a more general interest that transcends the results obtained here for somewhat artificial models. However, the extension of these methods to real fluids does not seem straightforward and deserves detailed study.

ACKNOWLEDGMENTS

Partial support from the DGES (Spain) through Grant No. PB97-1501 and from the Junta de Extremadura—Fondo Social Europeo through Grant No. IPR98C019 is gratefully acknowledged.

APPENDIX A: FIRST RETURN PROBABILITY IN THE GENERAL ROTATOR MODEL AND IN THE MIRROR MODEL

1. General rotator model

The rotator models defined in Sec. II for square and hexagonal Cayley trees can be easily extended to Cayley trees with any coordination number b. If the moving particle collides with a general rotator of this kind, it will be backscattered with probability β and deflected with probabilities α_1, α_2, ..., α_{b-1}, which are assigned to every direction in counterclockwise order for right rotators and clockwise order for left rotators. In a quenched configuration the branches growing from these directions have the corresponding returning probabilities $x_1,\ldots,x_{b-1}$, so that we can define a function $f(x_1,\ldots,x_{b-1})$ giving the probability of first return in this configuration, provided that the first scatterer visited is a rotator. Proceeding as in Sec. IV, it is easy to find that $f(x_1,\ldots,x_{b-1})$ is given by the right-hand side of Eq. (4.8), where the generalizations of the matrices $\boldsymbol{\alpha}$, X, M, and $\boldsymbol{\alpha}'$ are straightforward. In the particular case of isotropic scatterers ($\alpha_1=\alpha_2=\alpha_{b-1}=\beta=b^{-1}$), the result simplifies to

$$f(x_1,\ldots,x_{b-1})=\left(b-\sum_{i=1}^{b-1}x_i\right)^{-1}, \tag{A1}$$

which is the generalization of Eq. (4.12).

2. Mirror model

A line of reasoning parallel to that of Sec. IV shows that Eqs. (4.2), (4.4)–(4.6), and (4.8) are also valid for the mirror model on the square lattice, except that the matrix M now takes the form

$$\mathsf{M}=\begin{pmatrix} \beta & \alpha_3 & \alpha_2 \\ \alpha_3 & \beta & \alpha_1 \\ \alpha_2 & \alpha_1 & \beta \end{pmatrix} \tag{A2}$$

and $\boldsymbol{\alpha}'=\boldsymbol{\alpha}$. Also, x_1, x_2, and x_3 must be understood as the return probabilities along the branches with scattering probabilities α_1, α_2, and α_3, respectively. The final result is still given by Eq. (4.9), but now

$$g(x_1,x_2,x_3)=\alpha_1^2x_1(1-\beta x_2)(1-\beta x_3)+\alpha_2^2x_2(1-\beta x_1)(1-\beta x_3)+\alpha_3^2x_3(1-\beta x_1)(1-\beta x_2)+2\alpha_1\alpha_2\alpha_3[(1-\beta x_3)x_1x_2 + (1-\beta x_2)x_1x_3+(1-\beta x_1)x_2x_3]-[(\alpha_1^2-\alpha_3^2)^2-\alpha_2^2(2\alpha_1^2+2\alpha_3^2-\alpha_2^2)]x_1x_2x_3, \tag{A3}$$

$$\Delta(x_1,x_2,x_3)=(1-\beta x_1)(1-\beta x_2)(1-\beta x_3)-2\alpha_1\alpha_2\alpha_3x_1x_2x_3-\alpha_2^2x_1x_3(1-\beta x_2)-\alpha_1^2x_2x_3(1-\beta x_1)-\alpha_3^2x_1x_2(1-\beta x_3). \tag{A4}$$

In the case of what we have called the quasi-isotropic mirror model ($\alpha_1=\alpha_2=\beta=\frac{1}{3}$, $\alpha_3=0$), we simply have

$$f(x_1,x_2,x_3)=\frac{9-x_3(3+x_1+x_2)-x_1x_2+x_1x_2x_3}{27-9(x_1+x_2+x_3)+3x_1x_2+x_1x_2x_3}. \tag{A5}$$

In the trivial case of the deterministic mirror (Ruijgrok-Cohen) model ($\alpha_1=1$, $\alpha_2=\alpha_3=\beta=0$), one gets $f(x_1,x_2,x_3)=x_1$.

APPENDIX B: PERCOLATION THRESHOLD IN A CAYLEY TREE

The objective of this appendix is to prove by induction that the percolation threshold, x_B^c, predicted by the mean-field theory expressed in Eq. (4.18) is independent of n and takes the value $x_B^c=(b-2)/(b-1)$ for models defined on a Cayley tree with coordination number b. We only consider here the case $b=4$ for simplicity, but the generalization to any value of b is straightforward. Equation (4.17) for x in the mean-field theory of order $n=1$ can also be written as an equation for $y\equiv(x-x_B)/(1-x_B)$, the probability of first return along a path whose first scatterer is a rotator. If we define the function $\phi_1(y,x_B)\equiv y-h_1(y,x_B)$, where

$$h_1(y,x_B)\equiv x_B^3+(1-x_B)^3f(y,y,y)+x_B^2(1-x_B)[f(1,1,y)+f(1,y,1)+f(y,1,1)]+x_B(1-x_B)^2[f(1,y,y)+f(y,1,y)+f(y,y,1)], \tag{B1}$$

then Eq. (4.17) can be written as

$$\phi_1(y,x_B)=0. \tag{B2}$$

A mathematical solution of this equation for any value of x_B is $y=1$. This is in fact the *physical* solution if $x_B\geqslant x_B^c$ (where the percolation threshold x_B^c is here assumed unknown), while a root $y<1$ is the physical one in the interval $x_B<x_B^c$. This means that $\phi_1(y,x_B)=(1-y)\tilde{\phi}_1(y,x_B)$, where $\tilde{\phi}_1(y=1,x_B=x_B^c)=0$, so that $y\to1$ when $x_B\to x_B^c$ from below. Consequently, the following condition holds:

$$\left.\frac{\partial\phi_1(y,x_B)}{\partial y}\right|_{x_B=x_B^c,y=1}=0. \tag{B3}$$

This equation determines the percolation threshold, x_B^c. In order to calculate the derivative in (B3) we need the result

$$\left.\frac{\partial f(x_1,x_2,x_3)}{\partial x_i}\right|_{x_1=x_2=x_3=1}=1, \quad i=1,2,3, \tag{B4}$$

that follows from Eqs. (4.9)–(4.11). Equation (B4) implies

$$\left.\frac{\partial f(y,1,1)}{\partial y}\right|_{y=1}=1, \tag{B5a}$$

$$\left.\frac{\partial f(y,y,1)}{\partial y}\right|_{y=1}=2, \tag{B5b}$$

$$\left.\frac{\partial f(y,y,y)}{\partial y}\right|_{y=1}=3, \tag{B5c}$$

plus all the relations obtained from the above ones by permutation of the arguments of f. From these results and (B3) we get $1-3(1-x_B^c)=0$, which yields $x_B^c=\frac{2}{3}$.

The theory of order n is expressed through the relation

$$\phi_n(y,x_B)\equiv y-h_n(y,x_B)=0, \tag{B6}$$

where

$$h_n(y,x_B)\equiv\sum_{\mathcal{C}_n}\mathcal{P}(\mathcal{C}_n)f_{\mathcal{C}_n}(y). \tag{B7}$$

The condition for x_B^c is obtained from

$$\left.\frac{\partial\phi_n(y,x_B)}{\partial y}\right|_{x_B=x_B^c,y=1}=0. \tag{B8}$$

Now we will prove by induction that

$$\left.\frac{\partial h_n(y,x_B)}{\partial y}\right|_{y=1}=3^n(1-x_B)^n. \tag{B9}$$

First, Eq. (B9) is obviously true for $n=1$, as seen before. Next, since $h_n(y,x_B)$ represents the first return probability provided that the first scatterer visited is a rotator, we can decompose it in a similar way to that employed to write Eq. (4.17), so that Eq. (B7) is equivalent to

$$\begin{aligned}h_n(y,x_B)=&(1-x_B)^3\sum_{\mathcal{C}_{n-1}}\sum_{\mathcal{C}'_{n-1}}\sum_{\mathcal{C}''_{n-1}}\mathcal{P}(\mathcal{C}_{n-1})\mathcal{P}(\mathcal{C}'_{n-1})\mathcal{P}(\mathcal{C}''_{n-1})f(f_{\mathcal{C}_{n-1}}(y),f_{\mathcal{C}'_{n-1}}(y),f_{\mathcal{C}''_{n-1}}(y))+x_B(1-x_B)^2\\&\times\sum_{\mathcal{C}_{n-1}}\sum_{\mathcal{C}'_{n-1}}\mathcal{P}(\mathcal{C}_{n-1})\mathcal{P}(\mathcal{C}'_{n-1})[f(1,f_{\mathcal{C}_{n-1}}(y),f_{\mathcal{C}'_{n-1}}(y))+f(f_{\mathcal{C}_{n-1}}(y),1,f_{\mathcal{C}'_{n-1}}(y))+f(f_{\mathcal{C}_{n-1}}(y),f_{\mathcal{C}'_{n-1}}(y),1)]\\&+x_B^2(1-x_B)\sum_{\mathcal{C}_{n-1}}\mathcal{P}(\mathcal{C}_{n-1})[f(f_{\mathcal{C}_{n-1}}(y),1,1)+f(1,f_{\mathcal{C}_{n-1}}(y),1)+f(1,1,f_{\mathcal{C}_{n-1}}(y))]+x_B^3.\end{aligned} \tag{B10}$$

Thus, making use of Eq. (B4), we easily get

$$\left.\frac{\partial h_n(y,x_B)}{\partial y}\right|_{y=1}=3(1-x_B)\left.\frac{\partial h_{n-1}(y,x_B)}{\partial y}\right|_{y=1}. \tag{B11}$$

This completes the proof that Eq. (B9) holds for arbitrary n. Therefore, the solution of Eq. (B8) is $x_B^c=\frac{2}{3}$, regardless of the order n of the approximation.

Since Eq. (B4) also holds in the stochastic mirror model, the same result can be found in that case. By proceeding along similar lines in the case of models with a coordination number b, we obtain

$$\left.\frac{\partial h_n(y,x_B)}{\partial y}\right|_{y=1}=(b-1)^n(1-x_B)^n, \tag{B12}$$

which implies $x_B^c=(b-2)/(b-1)$. Near the critical point we can expand ϕ_n as

$$\begin{aligned}\phi_n(y,x_B)\approx&\frac{1}{2}\left.\frac{\partial^2\phi_n}{\partial y^2}\right|_{x_B=x_B^c,y=1}(y-1)^2+\left.\frac{\partial^2\phi_n}{\partial x_B\partial y}\right|_{x_B=x_B^c,y=1}\\&\times(y-1)(x_B-x_B^c),\end{aligned} \tag{B13}$$

where we have taken into account that $\phi_n(1,x_B)=0$, as well as Eq. (B8). Now Eq. (B6) yields

$$\begin{aligned}1-y\approx&(b-1)A_n(x_B^c-x_B),\quad A_n^{-1}\\&\equiv\frac{1}{2n}\left.\frac{\partial^2 h_n}{\partial y^2}\right|_{x_B=x_B^c,y=1},\quad n\geqslant 1.\end{aligned} \tag{B14}$$

Before concluding this appendix, it is worth taking advantage of Eq. (B10) to prove that the solution of Eq. (B6) is independent of n in some special cases. First, consider the deterministic rotator model. In that case, $f(x_1,x_2,x_3)=x_1x_2x_3$, so that Eq. (B10) becomes

$$h_n(y,x_B)=[x_B+(1-x_B)h_{n-1}(y,x_B)]^3. \tag{B15}$$

Thus, the solution of Eq. (B6) coincides with the solution of the cubic equation

$$y=[x_B+(1-x_B)y]^3, \tag{B16}$$

which is equivalent to the exact equation (1.7), for arbitrary n.

As a second application, let us consider models without backscatterers ($x_B=0$). Equation (B10) then becomes

$$h_n(y)=f(h_{n-1}(y),h_{n-1}(y),h_{n-1}(y)), \tag{B17}$$

so that Eq. (B6) is equivalent to

$$y=f(y,y,y) \tag{B18}$$

for arbitrary n. It is possible to prove [11] the equivalence between Eqs. (B18) and (3.15), where in the latter we must make $x_B=0$ and $z=(1+y)/(1-y)$.

Finally, let us consider the deterministic mirror model, in which case $f(x_1,x_2,x_3)=x_1$. Thus, Eq. (B10) yields

$$h_n(y,x_B)=x_B+(1-x_B)h_{n-1}(y,x_B) \tag{B19}$$

and Eq. (B6) is equivalent to

$$y=x_B+(1-x_B)y \tag{B20}$$

for any n, whose solution is (provided that $x_B\neq 0$) $x=y=1$.

[1] M. H. Ernst, in *Liquids, Freezing and Glass Transitions*, edited by J. P. Hansen, D. Levesque and J. Zinn-Justin (Elsevier Science Publishers, Amsterdam, 1991), pp. 43–143.
[2] *Discrete Kinetic Theory, Lattice Gas Dynamics and the Foundations of Hydrodynamics*, edited by R. Monaco (World Scientific, Singapore, 1989).
[3] J. R. Dorfman and P. Gaspard, Phys. Rev. E **51**, 28 (1995); P. Gaspard and J. R. Dorfman, *ibid.* **52**, 3525 (1995); J. R. Dorfman, M. H. Ernst, and D. Jacobs, J. Stat. Phys. **81**, 497 (1995); M. H. Ernst, J. R. Dorfman, R. Nix, and D. Jacobs, Phys. Rev. Lett. **74**, 4416 (1995); L. Acedo and M. H. Ernst, Physica A **247**, 91 (1997).
[4] A. J. H. Ossendrijver, A. Santos, and M. H. Ernst, J. Stat. Phys. **71**, 1015 (1993).
[5] D. Frenkel, F. van Luijn, and P. M. Binder, Europhys. Lett. **20**, 7 (1992).
[6] G. A. van Velzen and M. H. Ernst, J. Phys. A **22**, 4611 (1989); M. H. Ernst, G. A. van Velzen, and P. M. Binder, Phys. Rev. A **39**, 4327 (1989).
[7] H. van Beijeren and M. H. Ernst, J. Stat. Phys. **70**, 793 (1993).
[8] H. van Beijeren (private communication).
[9] J. M. F. Gunn and M. Ortuño, J. Phys. A **18**, L1035 (1985).
[10] D. Stauffer and A. Aharony, *Introduction to Percolation Theory* (Taylor and Francis, London, 1994).
[11] L. Acedo and A. Santos, J. Phys. A **30**, 6995 (1997).
[12] L. Acedo and A. Santos, Phys. Rev. E **50**, 4577 (1994).
[13] E. G. D. Cohen and F. Wang, J. Stat. Phys. **81**, 445 (1995).
[14] Th. W. Ruijgrok and E. G. D. Cohen, Phys. Lett. A **123**, 515 (1988); G. A. van Velzen, J. Phys. A **24**, 807 (1991).
[15] G. A. Velzen, J. Phys. A **23**, 4953 (1990); Ph.D. dissertation, University of Utrecht, 1990 (unpublished).